Biodiesel production from waste cooking oil in an oscillatory flow reactor. Performance as a fuel on a TDI diesel engine.

Juan Francisco García-Martín[a*], Carmen C. Barrios[b], Francisco-Javier Alés-Álvarez[a], Aida Dominguez-Sáez[b], Paloma Alvarez-Mateos[a]

[a]Department of Chemical Engineering, University of Seville, C/ Profesor García González, 1, 41012 Sevilla, Spain

[b]Environmental Department, Research Centre for Energy, Environment and Technology (CIEMAT), Avda. Complutense, 40, 28040 Madrid, Spain

*Corresponding author. *E-mail address:* jfgarmar@us.es

Abstract

This paper describes the biodiesel production from waste cooking oil (50% (v/v) olive oil/sunflower oil) in an oscillatory flow reactor (OFR) in batch mode. We mainly focused on the characteristics of the biodiesel and its performance as a fuel. First at all, we verified that biodiesel yield in OFR was higher than in stirred tank reactor (STR) under the same experimental conditions, and that composition and properties of the resulting biofuel did not depend on reactor type. Besides, biodiesel production in OFR took half the time than in STR. Subsequently, we modify some OFR operational parameters to assess their influence on biodiesel yield. The most suitable conditions were found to be 6:1 methanol to waste cooking oil molar ratio, 0.67 Hz oscillation frequency and 30 min reaction time. Finally, the biofuel obtained was tested in a 2.0 TDI 140 hp EURO4 engine installed on an engine test bench. Specific fuel consumption, particle size distribution and concentration of exhaust gas sample pollutants and were analysed running with commercial diesel, 50% (v/v) diesel/biodiesel blend (B50) and biodiesel (B100) in order to ensure the viability of using this biofuel in vehicle engines.

Keywords: Biodiesel; Engine performance; Exhaust emissions; Oscillatory flow reactor; Stirred tank reactor; Waste cooking oil.

1. INTRODUCTION

Biodiesel is a promising, renewable, clean-burning fuel which can be suitable to replace conventional diesel in boilers and internal combustion engines, without engine structural modifications and providing similar performance to that of a fossil fuel. Furthermore, biodiesel is highly biodegradable, has minimal toxicity, and its sulphur and aromatic compound emissions to the environment are almost nil. Nevertheless, it has some drawbacks such as higher fuel consumption and lower specific energy [1,2]. Biodiesel is composed of long-chain mono alkyl esters from vegetable oils, waste cooking oils (WCOs) or animal fats. The main problem in the production of biodiesel is the cost of the raw material that could be up to 75% of the total production cost [3], resulting in biodiesel prices 1.5 times higher than those of petroleum diesel [4]. One way to cut costs is the use of HORECA (hotels, restaurants and catering) WCOs as raw material, since these oils are 2-3 times cheaper than vegetable oils from crops or trees [5] and are already available as waste products. The catering industry produces around 400 000 tonnes of used cooking oils every year in Spain, of which around 58 000 tonnes are produced in the region of Andalusia. The use of WCOs for the production of biodiesel also reduces disposal management costs. In Andalusia, only around 34% of WCOs (20 000 tonnes) are currently collected and treated properly.

One of the main problems of WCOs is their chemical alteration by the reactions that occur during frying. Frying is a complex process in which numerous reactions promoted by three agents (water, oxygen and high temperature) provoke physical and chemical changes on plant oils. As a result, free fatty acids, diglycerides, oxidized monomers, dimers and polymers, and some volatile compounds (aldehydes, ketones, hydrocarbons, etc.) are generated during frying [6]. WCOs can also suffer degradation during storage, which can modify density, kinematic viscosity, acid number and water content [3]. Therefore, WCOs should be used as soon as possible

to avoid these chemical modifications. One of the advantages of the use of biodiesel is the reduction of greenhouse gas emissions compared to conventional diesel. Besides, the use of biodiesel significantly reduces carbon monoxide (about 44%), particulate matter (about 40%), and sulphur dioxide (100%) emissions [4], whereas the amount of nitrogen oxides can increase [6]. Biodiesel is commonly blended with conventional petroleum diesel to obtain B2 (2% biodiesel blended with 98% diesel), B5, B20 and B50. Pure biodiesel (B100) is also used as transportation fuel to lesser extent.

Biodiesel is typically obtained by a transesterification process, which involves the reaction of triglycerides with a short chain alcohol (methanol or ethanol) in the presence of an alkaline catalyst (mainly sodium or potassium hydroxide). Methanol is preferred over ethanol in commercial applications because of its lower cost. This process is reversible and consists of three consecutive reactions in which triglycerides are converted stepwise into: diglycerides, monoglycerides, and finally into glycerin, ultimately resulting three moles of esters (methyl or ethyl, depending on the short chain alcohol used) per mole glycerin obtained. The yield of the transesterification reaction is increased if alcohol is added in excess. WCOs not only contain triglycerides, but also free fatty acids and water. One way to remove them is to carry out an esterification process before the transesterification reaction. An esterification reaction is a reaction of free fatty acids with alcohol (generally methanol) to produce fatty acid methyl esters (FAME). Similarly to transesterification, esterification is also carried out in the presence of a catalyst. In this case, an acid catalyst is used (sulphuric acid).

Oscillatory flow reactor (OFR) consists of a tube containing baffles (orifice plates equally spaced). OFR operates with pulsed flow, which creates eddies in the vicinity of the baffles thereby improving heat transfer and mixing. When the piston advances, turbulence is created in the upstream holes. When the piston recedes, turbulence is

generated in the downstream direction below the baffle. The OFR technology is particularly good for liquid-liquid heterogeneous reactions such as transesterification because the recirculation flow increases the interfacial area in the liquid phase, which consequently enhances the rate of mass transfer. Furthermore, OFR provides better yields along with high oscillation amplitudes and low Strouhal numbers [7,8]. Therefore, OFR could achieve higher biodiesel yields than those obtained in stirred tank reactors.

The aim of this research was first to compare the efficiency in biodiesel production from HORECA WCO in a stirred tank reactor and in an oscillatory flow reactor under the same experimental conditions. Then the performance of the reactor which provided higher biodiesel yield was enhanced by modifying some operational parameters such as reactor loading, methanol to oil molar ratio, reaction time and oscillation frequency (this last one only for OFR). Finally, the performance of the biodiesel produced under the most favourable conditions was assessed in a 2.0 TDI 140 hp/4000 min^{-1} diesel engine. To this end, particle size distribution, concentration of the exhaust gas sample pollutants and specific fuel consumption of B50 and B100 were analysed and compared with those of commercial diesel under 9 engine operational conditions.

2. Materials and methods

2.1. Raw materials

150 L of a used mixture of olive oil and sunflower oil (1:1) were provided by catering services of CIEMAT (Research Center for Energy, Environment and Technology) and used throughout this research. In order to make a comparison with the performance of the biodiesel produced from this waste cooking oil (WCO), a petroleum fuel and the B50 obtained by mixing the produced biodiesel and this petroleum fuel were also assayed in the diesel engine. Table 1 shows the main fuel

properties of the commercial diesel (CD), B50 and B100 tested in the engine and sampling system.

TABLE 1

2.2. Oil conditioning

WCO was filtered due to the high amount of impurities lead such as leftover food, flour, etc. It may also contain a significant amount of water, so WCO was vacuum heated at 80 ºC for about 6 h to ensure total water removal, because water would affect the manufacturing process of biodiesel. Once the oil was clean, the acid index (AI) was measured, that is, the percentage of free fatty acids it contains. If this percentage is higher than 2.5% a pre-esterification reaction must be performed to transform the free fatty acids into methyl esters, because if the transesterification is directly carried out, they would become soap by reacting with caustic soda, thus decreasing significantly the process performance. The acid index of the raw WCO was 37%.

2.3. Biodiesel production

Two schemes were assayed, both of them in batch mode and using the same WCO and the same reagents in the same ratios. First at all, biodiesel was produced in an oscillatory flow reactor (OFR) at laboratory scale. Fig. 1 shows the flowchart of the biodiesel production in OFR. In the meantime, biodiesel production in a stirred tank reactor (STR) was performed to compare the performance of the OFR. The scheme for biodiesel production in STR was similar to that of OFR. Both pre-esterification and transesterification reactions were sequentially carried out in both reactors (Fig. 1).

FIGURE 1

2.3.1. Pre-esterification stage

Since AI of WCO was higher than 2.5%, it was esterified with methanol at 60 ºC using 1% (wt.) sulphuric acid as catalyst in the OFR. The resulting AI was 1.5%.

WCO with 1.5% AI was used as substrate for biodiesel production in both OFR and STR.

2.3.2. Transesterification procedure

Methanol to oil molar ratio of 6:1, temperature of 60 ºC and 1% (wt.) NaOH as catalyst were selected for biodiesel production. The reaction time was 60 and 30 min for STR and OFR, respectively (Table 2). These conditions were chosen based on previous research works [9,10] carried out by our research group in a stirred tank reactor where it was concluded that the optimum conditions were 6:1 methanol to oil molar ratio and 1% (wt.) catalyst (NaOH). This optimal oil to alcohol molar ratio has been suggested by other authors [7,8].

TABLE 2

1 kg WCO (1.5% AI) was mixed with methanol in a molar ratio 1:6 (256.96 mL methanol) and placed inside the reactor together with 1% (wt. WCO) sodium hydroxide. As aforementioned, reaction took place at 60 ºC and the residence time was 30 min for OFR and 60 min for STR. All the experiments were performed in triplicate. In principle, the transesterification reaction is a reversible reaction. However, the reverse reaction hardly occurs because the formation of glycerin as byproduct, which is immiscible with methyl esters and leads to the formation of a biphasic system formed by an upper phase of methyl esters (biodiesel) and a lower phase with glycerin. This causes separation of glycerin from the reaction mixture and therefore displacement of the reaction towards product formation reaching high conversions.

2.3.2.1. Oscillatory flow reactor (OFR)

The OFR used in this work consisted of a 15-L cylindrical reactor, with a heating jacket to keep the temperature to 60 ºC during the reaction. An air compressor was responsible for the pistons movement. Each cylinder of the tubular reactor contained 6 baffles, the separation between 2 consecutive baffles being 15.3 cm (Fig. 2). Each

plate-shaped baffle had a hole and was equidistant to the next disc, all discs having 5 cm diameter. Each plate had the same external diameter as the inner diameter of the reactor (14.4 cm). The thickness of the reactor wall was 3 cm and that of the baffle plates was 2 cm. The outer diameter of the reactor was 17.4 cm and it had a nominal height of 92.3 cm and a total height of 110 cm. The heating jacket was included in the thickness of 3 cm of the wall reactor.

FIGURE 2

The dimensionless numbers used to characterize the reactor were the oscillatory Reynolds number (Re_0) and the Strouhal number (St). Re_0 is obtained from the net flow Reynolds number ($Re_n = \frac{\rho\, v\, D}{\mu}$) and defined as:

$$Re_0 = \frac{\rho\, 2\, \pi\, f x_0\, D}{\mu}$$

where ρ is the fluid density (kg m^{-3}), v the net flow velocity (m s^{-1}), D the tube diameter (m), μ viscosity (kg m^{-1} s^{-1}), f oscillation frequency (s^{-1}), and x_0 the centre of the peak amplitude (m) [7]. The oscillatory Reynolds number stands for the mixing intensity, being $2\pi f x_0$ the maximum oscillatory velocity. Above Re_0 = 300, the higher the Re_0 value the more chaotic and intensely mixed the flow becomes.

The Strouhal number, defined as the ratio of the tube diameter to the oscillatory amplitude [7], describes eddy propagation and is calculated as follow:

$$St = \frac{D}{4\, \pi\, x_0}$$

2.3.2.2. Stirred tank reactor (STR)

Transesterification was carried out in a 5-L discontinuous stirred tank reactor at atmospheric pressure at 60 ºC. The inner diameter of STR was 15cm. Stirring was set to 500 rpm, diameter shovel being 6 cm. On the cover, the reactor was provided with a cooling system to prevent methanol losses.

The impeller Reynolds number (Re_i) was estimated as proposed by Oldshue [11].

$$Re_i = \frac{\rho\, N\, D_i^2}{\mu}$$

where N is the stirring speed (rps), D_i the impeller diameter (m), ρ the fluid density (kg m^{-3}) and μ the fluid viscosity (kg m^{-1} s^{-1}). The flow is laminar for $Re_i < 10$ and turbulent for $Re_i > 10^4$ [17].

2.3.3. Decantation stage

Once the reaction was complete, the reaction mixture was let to decant forming two phases, an upper phase of biodiesel with methanol and a minor lower phase, about 10% of the weight of the starting WCO, composed of glycerin and methanol excess.

2.3.4. Distillation stage

Once separated, both phases were distilled to recover the methanol. This step was performed at two separate phase's decantation; the aim was to recover the methanol excess in order to use it again and thereby minimize costs. For this purpose, a rotary evaporator was used with a vacuum pump and a water bath at 70°C, somewhat above the boiling point of methanol temperature. The pump used was a diaphragm vacuum pump model GM-100 with 200 mbar maximum vacuum, 230 V and 50 Hz voltage, 160 W power and 60 L min^{-1} speed. The obtained glycerin was stored for future reuse.

2.3.5. Filtration stage

Finally, biodiesel was passed through a purification tower where it was filtered by oak chips and alumina, thus eliminating soap and water, leaving biodiesel completely clean and in perfect conditions for use in fuel engines. The purifications tower had a capacity of 25 L and can purify 120 L of biodiesel a day.

2.4. Optimization of biodiesel production in OFR

Once verified that the oscillatory flow reactor provides better efficiency, the operating conditions were optimized by varying the following parameters: methanol to WCO molar ratio, residence time and piston speed. All tests were performed in

duplicate and in all cases the same WCO was used. Experimental conditions are shown in Table 3.

TABLE 3

2.5. Engine and sampling system

The engine test bench used was made up of a diesel engine and dynamometer (SCHENCK W150) controlled by a HORIBA's SPARC system. The diesel engine tested was a 2.0 TDI 140 hp/4000 min^{-1}, Euro 4, four stroke and direct injection. The technical specification details of the engine are described in Table 4. The exhaust gas post-treatment system consisted of a diesel oxidation catalyst. Particle size distribution data was measured using an engine exhaust particle sizer 3090 (TSI Inc., USA) and a rotating disc raw gas diluter Testo MD19-2E (Testo SE & Co. KGaA, Germany), using a first hot dilution (150 ºC, 1:1695) and a second cold dilution (room temperature, 1:2) as described elsewhere [12,13]. The control of thermodynamic properties of the sample prevents particle nucleation from the volatile compounds present in the exhaust gas. The dilution system and particle sampling has been amply demonstrated and illustrated in the authors' previous publications [14-15]. An OBS 2200 on-board emission measurement system (HORIBA Inc., USA) was used to measure the concentrations of the regulated exhaust gas sample pollutants. The equipment set-up is shown in Fig. 3. Additionally, different operating parameters of the engine were recorded, such as speed, torque, throttle position, intake air temperature, temperature of the exhaust gas, flow of exhaust gas, percentage of exhaust gas recirculation, fuel temperature, specific fuel consumption (through the instantaneous consumption and the effective power) and brake thermal efficiency (considering the lower heating value of each fuel). The measurement was carried out continuously and the data was recorded at 1 Hz.

TABLE 4

FIGURE 3

Regulated emissions and particle emissions in number and size distribution were measured in nine stable conditions (1500, 2250, and 3000 min^{-1} at 15%, 30% and 45% engine load) as illustrated in Table 5. Tests were conducted in an engine test bench with B50 (50% biodiesel and 50% pure petroleum fuel), B100 (100% biodiesel) and commercial diesel (CD). Engine load percentage was calculated regarding the maximum engine torque at each speed using CD. Engine load was controlled by setting the desired engine torque in the engine test bench, from which the engine speed and engine torque were controlled. Operational conditions are shown in Table 5. Each operational condition was maintained for one minute and monitored at 1 Hz. Only 30 data were used for the analysis, deleting the first 25 and the last 5 data, thus ensuring that the engine and emissions were stabilized. Three tests were performed with each operating condition and each fuel, randomly and automatically controlled, in order to ensure repeatability of measurements despite all possible outliers. Each fuel blend change was preceded by the execution of an intermediate cleaning test for a minute under steady state.

TABLE 5

2.6. Analytical methods

Biodiesel density at 15 ºC and boiling point determinations were carried out following UNE-EN ISO 3675 and UNE-EN ISO 12185 standards, and UNE-EN 14213 standard, respectively. Biodiesel elemental analysis was carried out in a CHNS-932 elemental analyser (LECO).

Fatty acid methyl esters (FAME) percentages were calculated following UNE-EN 14103:2011 and UNE-EN ISO 12966-1:2015 standards. The percentages of FAME in the sample were determined by gas chromatography using methyl heptadecanoate as internal standard. An HP 5890 series II gas chromatograph equipped with a

SP2380 capillary column (60 m × 0.25 mm internal diameter × 0.25 μm film thickness) was used. The column temperature was set to 172 ºC and then the temperature program ramped from to 200 ºC at 1.5 ºC min^{-1}. The injection was operated in splitless mode, the injector and detector temperatures being 225 °C and 250 °C, respectively. FAME were identified by mass spectrometry, comparing the spectra with those in the database for this type of compounds (Wiley, NIST).

The iodine value was determined in biodiesel obtained by both STR and OFR by following UNE-EN 14111. It represents the grams of iodine that react with 100 g of sample and is an indicator of the total unsaturation of biodiesel.

The lower heating value was calculated following ASTM D240-09 standard using a Parr 1341 plain jacket calorimeter bomb (Parr Instrument Company). Viscosity of biodiesel was measured by a HAAKE MARS modular advanced rheometer system (Thermo Electron Corporation). Cetane number (CN) of biodiesel from the FAME composition was calculated using the equation proposed by Bamgboye and Hansen [16]:

$$CN = 61.1 + 0.088x_2 + 0.133x_3 + 0.152x_4 – 0.101x_5 – 0.039x_6 – 0.243x_7 – 0.395x_8$$

where x_2, x_3, x_4, x_5, x_6, x_7 and x_8 stand for myristic, palmitic, stearic, palmitoleic, oleic, linoleic and linolenic acid methyl esters percentages (% wt.), respectively, in the biodiesel fuel (Table 6).

TABLE 6

3. Results and Discussion

3.1. Comparative analysis between OFR and STR

In order to compare the FAME yields achieved, biodiesel yield (% wt.) was defined as the weight of the whole FAME obtained per weight of WCO used for

291 transesterification. In this section, a comparative study is detailed between the most
292 common biodiesel production system (STR) and the OFR. Both systems worked in
293 bath, and used the same WCO and the same reagents in the same ratios. The
294 experimental conditions of the experiments are shown in Table 2. The Reynolds
295 number obtained for the stirred tank was Re_i = 2100, while for the oscillatory flow
296 Re_0 = 1050 and the Strouhal number was 0.11. This Re_i value means the flow was
297 right in the transitional flow regime (neither laminar nor turbulent) when working
298 with the STR. For OFR, Re_0 values between 100 and 300 indicate that vortices are
299 symmetrically generated within each baffle cavity during each oscillation of the fluid
300 [18]. When Re_0 increases further, vortices are no longer symmetrical. As the Re_0
301 obtained for OFR was 1050, the flux inside the reactor was intensely mixed and
302 chaotic.
303 OFR achieved higher biodiesel yield (72.50% wt.) than STR (63.50% wt.) and
304 required half the time (Table 2) to reach it. Biodiesel obtained from both reactors
305 were analysed in terms of FAME composition, cetane number, density at 15°C,
306 boiling point, LHV and viscosity. Table 6 illustrates the fatty acid composition of
307 biodiesel obtained from STR and OFR, being the showed data the average from three
308 replicas. As can be seen, biodiesel obtained by both reactors had the same FAME
309 composition and physicochemical properties. This is because, regardless of the
310 reactor used, the analysed parameters depend primarily on the starting oil. The cetane
311 numbers calculated (52.78 for STR and 53.73 for OFR) were slightly higher than that
312 of CD (51.3; Table 1). Biodiesel usually has cetane number higher than petroleum
313 diesel fuel, which in theory provides better combustion efficiency. As illustrated in
314 equation applied for cetane number calculation [16], cetane number of biodiesel is
315 largely affected by its FAME composition.
316 *3.2. OFR performance enhancement*

In order to increase the biodiesel yield in the OFR, the effect of methanol to WCO molar ratio (6:1, 8:1 and 10:1), residence time (20 and 30 min), oscillation frequency (0.33 and 0.67 Hz) and WCO loading (2 and 3 kg) was assessed. Experiments were carried out using the one variable change at a time approach, and therefore interaction effects were not investigated. The temperature was fixed to 60 ºC. These experimental conditions are summarized in Table 3. Each experiment was performed in duplicate. The preliminary comparison with the STR was carried out with 1 kg WCO loading due to the limited volume of the STR (5 L). As the internal volume of the OFR was 15 L, this set of experiments was performed with higher WCO loadings (2 and 3 kg). From the biodiesel yields showed in Table 3 it can be concluded that the most suitable conditions for biodiesel production in OFR were the same than those assayed in the comparative study OFR vs STR (but using 2 kg WCO loading instead of 1 kg), which led to 78.8% (wt.) conversion of WCO to FAME.

With regards to the operational parameters, reaction time exerted the highest influence on efficiency, as it can be clearly observed by comparing experiments 2 and 3 (Table 3). The lowest biodiesel yield (54.6% wt.) was obtained when the reaction time was set to 20 min (run 7). The whole experiments performed with 20 min reaction time achieved lower biodiesel yields than those carried out for 30 min (Table 3). As for reactor loading, no differences were found when using 2 or 3 kg WCO (runs 1 and 2). 2 kg was used instead of 3 kg WCO because increasing the reactor loading could lead to overpressure or leaks on the top of the reactor. The WCO to methanol molar ratio which provided the highest yield (78.8% wt.) was 1:6, which is in agreement with our previous results with other raw materials in STR [10-11]. By comparing run 2 with 4, run 5 with run 6, and run 7 with run 9, it was found that biodiesel yield was improved by increasing the oscillation frequency (i.e.: increasing piston strokes per second and increasing Re_0), leading to greater turbulence and thus increasing mass and heat transfer. Finally, it was verified that the

use of recycled methanol (recovered from the distillation step after transesterification process) did not exert any negative influence on biodiesel yield. The difference in efficiency between experiments 9 and 10 was almost nil (Table 3). The use of recycled methanol can have major consequences in the feasibility of biodiesel production, due to the reduction in reagent costs.

3.3. Specific fuel consumption (SFC)

The lowest specific fuel consumption was observed with commercial diesel (CD) (Fig. 4a). When biodiesel was assayed, an increase in the specific fuel consumption was observed, mainly due to the decrease of the lower heating value (LHV) of biodiesel. The LHV of the biodiesel was approximately 8% lower than that of CD, which resulted in an increase of SFC depending on the percentage of biodiesel. B100 had the highest values of SFC, up to 12% more than commercial diesel. On the other hand, the higher viscosity of biodiesel (3.92 cSt) hindered the atomization and vaporization of fuel and worsened the combustion process. Regardless of the percentage of biodiesel in the fuel, the SFC decreased with fuel load for the same engine speed, since the engine was running nearest to the optimal operating zone (Fig. 4a). In the case of biodiesel, the SFC increased, compared with CD, under all engine operation conditions. By contrast, under conditions far from the optimal effective efficiency (stable conditions between 1500 min^{-1} and 3000 min^{-1}) the SFC of biodiesel increased to a lesser extent. The SFC increase of B50 was lower than that of B100 due to the higher LHV value of B50. At low engine speed and low fuel load (1500 min^{-1} and 15% load) the exhaust gas recirculation (EGR) was very high so that combustion efficiency and SFC got worse. At medium engine speed (2000 to 2500 min^{-1}), EGR was lower and the time required for complete combustion decreased with increasing engine speed, so that the addition of biodiesel, thus reducing LHV of the fuel, resulted in greater SFC. At high engine speed without EGR, the decreasing time for the combustion process to occur is compensated by the

increase of the combustion efficiency for B50 and B100, so that the increase of SFC did not occur in the same proportion than at medium loads (Fig. 4a).

FIGURE 4

3.4. Total particle number concentration in the size range 5.6 to 560 nm

According to other studies [13], when the percentage of biodiesel is higher than 30%, the total particle number concentration decreases due to the increase of oxygen in the fuel blend. In many WCO-derived biodiesel studies, significant reductions in total particle number concentration, especially particles in accumulation mode, have been observed in comparison with commercial diesel [19-21]. The average values of the total number of particles under all assayed conditions were $8.35 \cdot 10^{7}$ # cm^{-3}, $5.20 \cdot 10^{7}$ # cm^{-3} and $7.60 \cdot 10^{-7}$ # cm^{-3} for CD, B50 and B100, respectively. Therefore, a decrease of 38% of total particle number concentration was found by using B50 instead of CD. Interestingly, the use of B100 only led to a reduction in particle number concentration of 9% in comparison to commercial diesel. The harmful effects on health of emitted particles from diesel engines is due to the smallest emitted particles (10-30 nm). These small particles get trapped in the lungs and can pass through them into the blood stream [6]. From this point of view, the addition of biodiesel to petroleum diesel is an advantage. The particle number size distribution of the assayed engine showed unimodal or bimodal log-normal distributions depending on the condition or fuel used. The use of B100 caused high particle number emissions in nucleation mode in all operating conditions tested, and the geometric mean diameter (GMD) in accumulation mode decreased with the increase of biodiesel blend. According to other authors [22], three mechanisms could lead to a higher formation of nucleation mode particles: First, new nucleation particles may appear due to high super-saturation. Second, lower volatility and higher viscosity of biodiesel could lead to a slower evaporation and air mixing in a local area of combustion chamber, which is not equal compared with pure diesel fuel and this may

cause volatile compounds increase. And finally, oxygen content of biodiesel fuel can cause carbonaceous particle changing from fine size to ultrafine size or, even, nano-particle size. The nucleation particle formation should be linked to the higher semi-volatile emissions and the lower soot mode of biodiesel fuel, which promotes homogeneous nucleation [23]. This effect is more noticeable in pure biodiesel (B100). In accordance with to other authors' results with B100 (WCO-derived biodiesel), the particles in nucleation mode reach values of 10^8, twice that obtained with B50 and pure diesel, this phenomenon occurring under high load conditions [24]. The optimal emissions of particle in the size range of 5.6-560 nm were found using B50 under all the assayed engine conditions in comparison with the particle number emission using conventional diesel (Fig. 4c). The absolute difference between both biofuels with regards to particle number emissions was higher with low engine load percentage (15% of maximum engine torque). By increasing the load, the mixture was richer, and the use of biofuels increased the particle emissions in nucleation mode (Fig. 4d and Fig. 5), thereby increasing the total number of particles.

FIGURE 5

3.5. Geometric mean diameter (GMD) of accumulation particles

The geometric mean diameter (GMD) of the emitted particles with particle diameter higher than 24 nm depended on the blend used and on the operating conditions. The GMD specially decreased with increasing engine speed (Fig. 4e), since the accumulation phenomena is less likely to occur [14]. In terms of fuel used, the general trend was that GMD decreased when increasing the percentage of biodiesel in the fuel [15,25]. The addition of WCO-derived biodiesel in different blend proportions in a 4-cyclinder natural-aspirated direct-injection diesel leads to smaller GMD and decrease in total particle number due to less soot nuclei formed and more complete combustion in comparison with diesel fuel [26]. The increasing of the percentage of biodiesel caused a decrease of the percentage of carbon and an increase

425 of that of oxygen, favouring the reduction of elemental carbon and decreasing
426 accumulation and agglomeration phenomena. As a result, the GMD decreased with
427 the increase of biodiesel percentage in the fuel (Fig. 5).

428 *3.6. Nitrogen oxides (NOx)*

429 According to the most studies on the use of WCO methyl esters in compression
430 ignition engines, the NOx emission increases [26-28]. Therefore, NOx emissions
431 significantly depend on the engine type, on the used fuel and on the operational
432 conditions of the engine used. The NOx dependence on operative condition was
433 greatly influenced by the exhaust gas recirculation (EGR). Under a specific operation
434 condition, defined by the engine speed and constant engine torque (Table 5), an
435 increase in the EGR percentage reduced the concentration of NOx and increased the
436 total particle number [15]. The EGR control system was able to maintain a constant
437 nitrogen oxide emission until reaching the barrier of 2200 min^{-1} (70 km h^{-1}). From
438 that point on, the need for more engine power so as to attain higher speeds reduced,
439 or even nullified, the EGR proportion, causing a dramatic rise in the NOx emission
440 (Fig. 4b). Regarding the influence of biodiesel on the fuel, the NOx emissions,
441 according to other authors [29,30], increased with the proportion of biodiesel in the
442 blend, due to two phenomena: (a) The increase of iodine value makes the biodiesel
443 more unsaturated and (b) the higher percentage of oxygen increases the temperature
444 within the combustion chamber and supplies additional oxygen for the formation of
445 NOx. Fig. 6 shows the NOx emission dependence with exhaust temperature (and
446 therefore combustion temperature) and fuel used. Both B50 and B100 exceeded the
447 mean NOx emissions of the reference fuel (CD). A general trend was the increase of
448 NOx emissions with the use of biodiesel (Fig. 4b), due to the aforementioned exposed
449 causes. Besides, the lower LHV of biodiesel (compared with that of commercial
450 diesel) forced the electronic engine control unit to reduce the proportion of EGR so

as to maintain the operational conditions required by the engine. The proportion of biodiesel in the blend was related to the general trend of EGR percentage reduction.

FIGURE 6

3.7 Carbon monoxide (CO) and total hydrocarbons (THC)

There were not differences in the THC emission among the three fuels tested. All the experiments were conducted in hot engine conditions, therefore THC values were very low and ranging from 6 to 15 mg kg^{-1}.

The CO emission values were also very low for all experimental conditions (Fig. 7). However, B50 and B100 decreased the CO emission with respect to CD for all the experimental conditions. This is due to the more complete combustion of biodiesel because its additional oxygen content and the increase in cetane number [31].

FIGURE 7

CONCLUSIONS

The use of OFR for waste cooking oil transesterification provided higher biodiesel yield (72.5%) than STR (63.5%) under the same experimental conditions in bath mode. Besides, OFR required half the time (30 min) than STR (60 min). The obtained biodiesels by both reactors had similar FAME composition and physicochemical properties (cetane number, density, boiling point, lower heat value and viscosity) because the properties of biodiesel solely depend on the oil used for transesterification. The most suitable experimental conditions for our 15-L OFR were 2 kg waste cooking oil loading, 6:1 methanol to waste cooking oil molar ratio, 0.67 Hz oscillation frequency and 30 min reaction time, the biodiesel yield reaching a maximum of 78.8%. The use of either recycled or commercial methanol did not make difference on biodiesel yield. When applied to vehicle engines in form of B50 and B100, biodiesel increased the specific fuel consumption, compared to petroleum diesel, mainly due to smaller LHV of biodiesel. Therefore, the highest specific fuel consumption was found for B100. In addition, the use of biodiesel increased the

engine NOx emissions. By contrast, total particle number and GMD decreased with the increase of biodiesel percentage in the fuel due to the increase of oxygen in the fuel blend. Interestingly, B50 was the most effective fuel for reducing the total particle number concentration (38% less than CD in the size range 5.6-560.0 nm). Because of this, and since NOx emissions and SFC of B50 were lower than those of B100, it can be concluded than B50 was the most suitable fuel for diesel engine from between the two assayed biofuels (B50 and B100) produced from WCO (1:1 olive oil:sunflower oil) in OFR.

ACKNOWLEDGEMENTS

This work was supported by the European Union Funds under grant LIFE 13-Bioseville ENV/1113.

REFERENCES

[1] Chattopadhyay S, Sen R. Fuel properties, engine performance and environmental benefits of biodiesel produced by a Green process. Appl Energ 2013;105:319–326.

[2] Xue J, Grift TE, Hansen AC. Effect of biodiesel an engine performances and emisions. Renew Sust Energ Rev 2011;15(2):1098–1116.

[3] Khalid A, Azman N, Zakaria H, Manshoor B, Zaman I, Sapit A, Leman AM. Effects of storage duration on biodiesel properties derived from waste cooking oil. Appl Mech Mater 2014;554:494–499.

[4] Talebian-Kiakalaieh A, Amin NAS, Mazaheri H. A review on novel processes of biodiesel production from waste cooking oil. Appl Energ 2013;104:683–710.

[5] Demirbas A. Progress and recent trends in biodiesel fuels. Energ Convers Manage 2009(1);50:14–34.

503 [6] Kappos AD, Bruckmann P, Eikmann T, Englert N, Heinrich U, Hoppe P, Koch
504 E, Krause GH, Kreyling WG, Rauchfuss K, Rombout P, Schulz-Klemp V, Thiel WR,
505 Wichmann HE. Health effects of particles in ambient air. Int J Hyg Envir Heal
506 2004(4);207:399–407.
507 [7] Zheng M, Sketon RL, Mackley MR. Biodiesel reaction screening using
508 oscillatory flow meso reactors. Process Saf Environ 2007;85(5):365–371.
509 [8] Harvey AP, Mackley MR, Seliger, T. Process intensification of biodiesel
510 production using a continous oscillatory flow reactor. J Chem Technol Biot
511 2003;78(2-3):338–341.
512 [9] Lama-Muñoz A, Álvarez-Mateos P, Rodríguez-Gutiérrez G, Durán-Barrantes
513 MM, Fernández-Bolaños J. Biodiesel production from olive-pomace oil of steam-
514 treated alperujo. Biomass Bioenerg 2014;67:443–450.
515 [10] Marín PJP, Mateos FB, Mateos PÁ. Use of residual soapstock from the refining
516 of edible vegetable oils to make biodiesel. Grasas Aceites 2003;54:130–137.
517 [11] Oldshue JY. Power correlations and effects of mixing environment. In: Fluid
518 mixing technology. Chemical Engineering McGraw-Hill Pub. Co., New York. 1983;
519 51–63.
520 [12] Johnson T, Caldow R, Pocher A, Mirme A, Kittelson DB. 2004. A new electrical
521 mobility particle sizer spectrometer for engine exhaust particle measurements. SAE
522 Tech Paper 2004-01-1341.
523 [13] Kasper M. The number concentration of non-volatile particles, design study for
524 an instrument according to the PMP recommendations. SAE Tech Paper 2004-01-
525 0960.
526 [14] Barrios CC, Dominguez-Saez A, Rubio JR, Pujadas M. Development and
527 evaluation of on-board measurement system for nanoparticle emissions from diesel
528 engine. Aerosol Sci Tech 2011;45(11):570–580.

529 [15] Barrios CC, Domínguez-Sáez A, Martín C, Álvarez P. Effects of animal fat
530 based biodiesel on a TDI diesel engine performance, combustion characteristics and
531 particle number and size distribution emissions. Fuel 2014;117:618–623.
532 [16] Bamgboye AI, Hansen AC. Prediction of cetane number of biodiesel fuel from
533 the fatty acid methyl ester (FAME) composition. Int Agrophys 2008;22(1):21–29.
534 [17] Geankoplis CJ, Transport Processes and Unit Operations, Prentice-Hall Int.
535 (1993) 1–937.
536 [18] Ni X, Gough P. On the discussion of the dimensionless groups governing
537 oscillatory flow in a baffled tube. Chem Eng Sci 1997;52:3209–3212.
538 [19] Man XJ, Cheung CS, Ning Z, Yung KF. Effect of waste cooking oil biodiesel
539 on the properties of particulate from a DI diesel engine. Aerosol Sci Technol
540 2015;49(4):199e209.
541 [20] Betha R, Balasubramanian R. A study of particulate emissions from a stationary
542 engine fuelled with ultra-low sulfur diesel blended with waste cooking oil-derived
543 biodiesel. J Air Waste Manage Assoc 2013;61:1063–1069.
544 [21] Lu T, Cheung CS, Huang Z. Influence of waste cooking oil biodiesel on the
545 particulate emissions and particle volatility of a DI diesel engine. Aerosol Air Qual
546 Res 2013;13(1):243e54.
547 [22] Tan P, Lou D, Hu Z, 2010. Nucleation mode particle emissions from a diesel
548 engine with biodiesel and petroleum diesel fuels. SAE Tech Paper 2010-01-0787.
549 [23] Fontaras G, Tzamkiozis T, Ntziachristos L, Samaras Z. Biodiesel (soy-bean
550 FAME) effect on particulate and gaseous pollutants from a passenger car. In:
551 European Aerosol Conference, Karlsruhe, Germany, 2009 Abstract T112A01.
552 [24] Feng Q, Lou D, Tan P, Hu ZY. Effect of biodiesel blends on ultrafine particle
553 number concentration from diesel passenger car under real-world driving conditions.
554 Int Proc Chem Biol Environ Eng 2014;69:81–88.

555 [25] Di Y, Cheung CS, Huang Z. Experimental investigation on regulated and
556 unregulated emissions of a diesel engine fueled with ultra-low sulfur diesel fuel
557 blended with biodiesel from waste cooking oil. Sci Total Environ 2009;407(2):835–
558 846.
559 [26] Cheung CS, Man XJ, Fong KW, Tsang OK. Effect of waste cooking oil biodiesel
560 on the emissions of a diesel engine. Energy Proc 2015;66:93–6.
561 [27] Kathirvel S, Apurba L, Muthuraman S. Exploration of waste cooking oil methyl
562 esters (WCOME) as fuel in compression ignition engines: A critical review. Eng Sci
563 Technol 2016;19(2):1018–1026.
564 [28] Gopal KN, Pal A, Sharma S, Samanchi C, Sathyanarayanan K, Elango T.
565 Investigation of emissions and combustion characteristics of a CI engine fueled with
566 waste cooking oil methyl ester and diesel blends. Alexandria Eng J 2014;53:281–
567 287.
568 [29] Lapuerta M, Armas O, Rodríguez-Fernández J. Effect of the degree of
569 unsaturation of biodiesel fuels on NOx and particulate emissions. SAE Int J Fuels
570 Lubr 2009;1(1):1150–1158.
571 [30] Canakci M, Van Gerpen JH. Comparison of engine performance and emissions
572 for petroleum diesel fuel, yellow grease biodiesel, and soybean oil biodiesel. T ASAE
573 2003;46(4),937–944.
574 [31] Lapuerta M, Armas O, Fermandez JR. Effect of biodiesel fuels on diesel engine
575 emissions. Prog Energy Combust Sci 2008;34:198–223.

Table 1. Main fuel properties of the commercial diesel (CD) and biodiesel used.

Property	**CD**	**B50**	**B100**
Formula	$C_{12}H_{22.6}$	$C_{22}H_{41}O$	$C_{10.5}H_{19.3}O$
Cetane Number	51.3 ± 3.3	56.9 ± 2.7	62.5 ± 2.2
Viscosity at 40 ºC (cSt)	2.9 ± 0.18	3.4 ± 0.19	3.9 ± 0.20
Density at 15 ºC (kg m^{-3})	840 ± 1.8	861 ± 1.8	882 ± 1.8
Stoichiometric fuel/air ratio (kg kg^{-1})	1/14.5	1/12.1	1/9.3
Latent heat of vaporization (kJ kg^{-1})	270 ± 11.5	-	-
Lower mass heating value (kJ kg^{-1})	40377 ± 146	32349 ± 109	24231 ± 72
Flash point (ºC)	40 ± 1.3	98 ± 1.2	156 ± 1.1

Table 2. Operational parameters for biodiesel production comparison between OFR and STR.

Reactor	T (ºC)	time (min)	WCO (kg)	MeOH:WCO	Catalyst (% wt.)	Oscillation frequency (Hz)	Re_i	Re_0	St	Biodiesel yield (%wt.)
STR	60	60	1	6:1	1		2100			63.50 ± 0.75
OFR	60	30	1	6:1	1	0.33		1050	0.11	72.50 ± 1.50

Table 3. Experimental conditions and results for biodiesel production in OFR.

Run	WCO (kg)	MeOH:WCO	Residence time (min)	Oscillation frequency (Hz)	Biodiesel yield (%wt.)	Re_0	St
1	3	10:1	30	0.33	73.5 ± 1.3	1050	0.11
2	2	10:1	30	0.33	73.0 ± 1.3	1050	0.11
3	2	10:1	20	0.33	57.5 ± 0.65	1050	0.11
4	2	10:1	30	0.67	74.2 ± 1.5	2100	0.11
5	2	6:1	30	0.33	68.2 ± 0.80	1050	0.11
6	2	6:1	30	0.67	78.8 ± 1.7	2100	0.11
7	2	8:1	20	0.33	54.6 ± 0.64	1050	0.11
8	2	8:1	30	0.67	72.8 ± 1.3	2100	0.11
9	2	8:1	20	0.33	63.6 ± 0.73	1050	0.11
10	2	8:1*	20	0.33	63.2 ± 0.75	1050	0.11

*Reusing the methanol distilled in the previous run

Table 4. Test engine specifications.

Model	2.0 TDI Volkswagen
Year	2005 (Euro 4)
Configuration	In-line 4-cylinder
Air intake	Turbocharged
Fuel injection	Direct Injection (injector pump, 6 holes 0.117 µm)
Displacement	2.0 L
Max Torque	320 Nm/1750-2500 min^{-1}
Max Power	103 kW/4000 min^{-1}
Compression ratio	18
EGR	Yes
DPF	No

Table 5. Engine torque at each operational condition.

		Maximum load percentage		
		15%	30%	45%
Engine	1500 min^{-1}	29 Nm	58 Nm	86 Nm
speed	2250 min^{-1}	54 Nm	108 Nm	162 Nm
	3000 min^{-1}	52 Nm	103 Nm	155 Nm

Table 6. FAME composition, elemental composition and physicochemical properties of biodiesel obtained in STR and OFR.

		STR	OFR
FAME (%wt.)	Lauric acid	0.46 ± 0.12	0.46 ± 0.12
	Myristic acid	1.21 ± 0.32	1.21 ± 0.32
	Palmitic acid	36.67 ± 5.7	36.60 ± 5.5
	Stearic acid	6.29 ± 0.31	6.27 ± 0.23
	Palmitoleic acid	0.00	0.00
	Oleic acid	43.83 ± 2.7	43.85 ± 2.0
	Linoleic acid	11.55 ± 2.5	11.61 ± 2.4
	α-Linolenic acid	0.00	0.00
Elemental composition	C (%wt.)	78.12 ± 0.28	78.14 ± 0.29
	H (%wt.)	11.82 ± 0.050	11.89 ± 0.051
	N (%wt.)	0.098 ± 0.0051	0.096 ± 0.0052
	S (%wt.)	0.071 ± 0.0068	0.068 ± 0.0066
	O (%wt.)	9.88 ± 0.27	9.89 ± 0.29
Properties	FAME (%wt.)	99.60 ± 0.11	99.70 ± 0.10
	Cetane number	62.52 ± 2.5	62.49 ± 2.2
	Boiling point (ºC)	343 ± 1.5	345 ± 1.5
	Density at 15 ºC (kg m^{-3})	884 ± 1.5	882 ± 1.8
	Lower heating value (kJ kg^{-1})	24223.1 ± 71	24231.4 ± 72
	Viscosity at 40 ºC (cSt)	3.92 ± 0.21	3.92 ± 0.20
	Iodine value	77.7 ± 2.0	77.7 ± 2.0

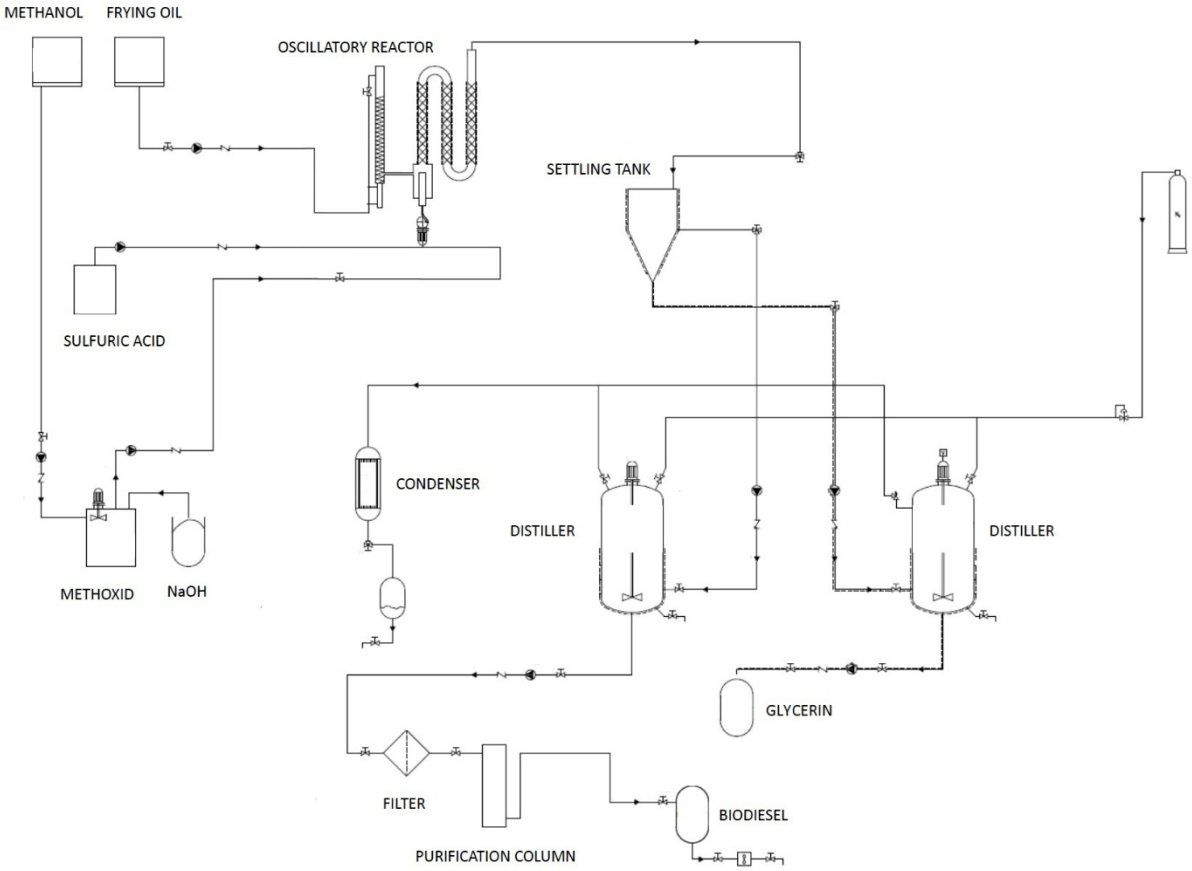

Figure 1. Flowchart of the biodiesel production.

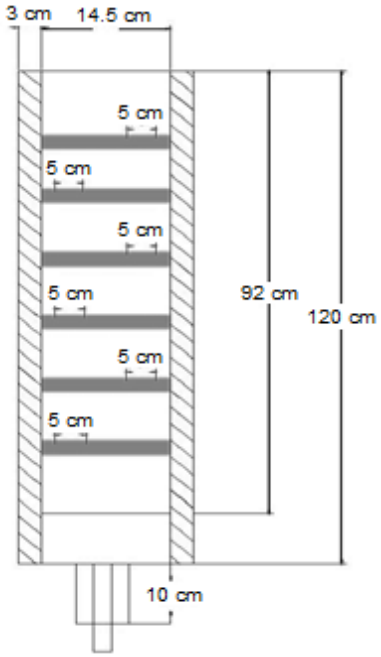

Figure 2. Baffles of OFR.

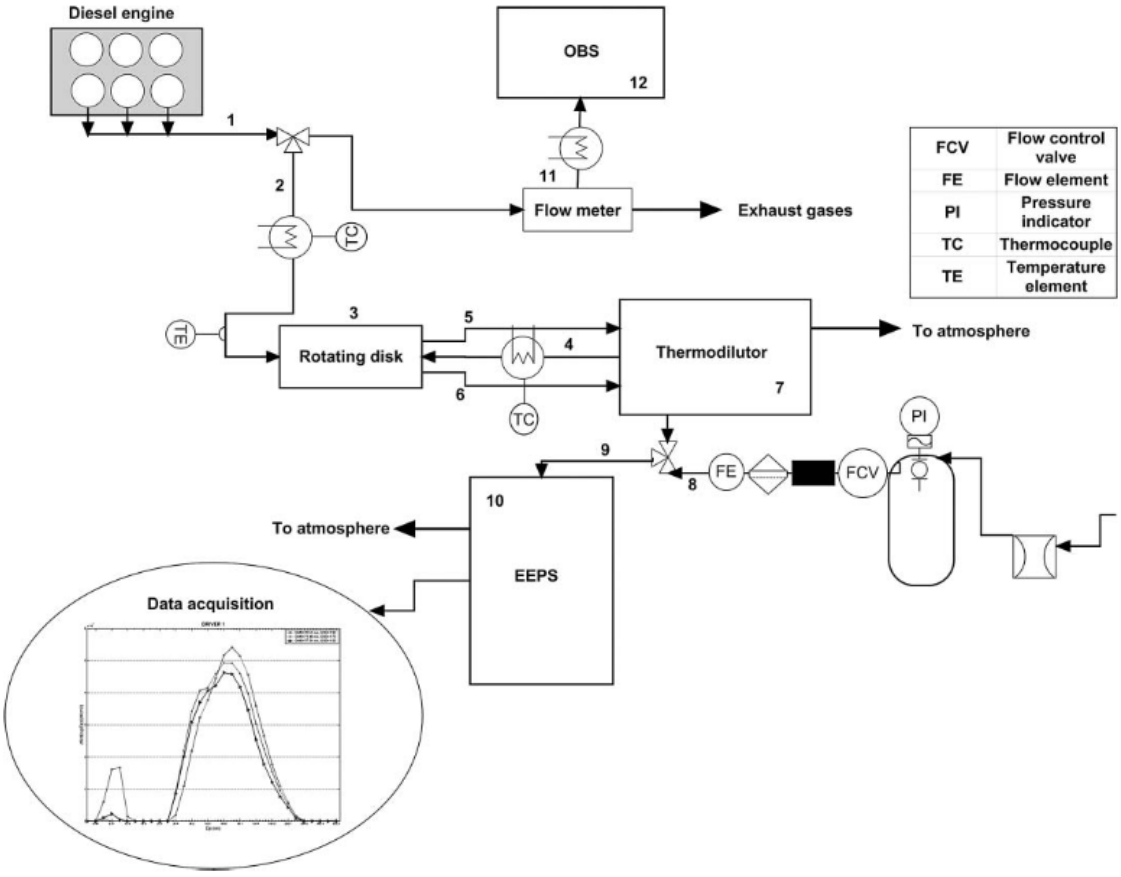

Figure 3. Set-up for particle size distribution and gases measurement. (1) Exhaust pipe; (2) heater pipe; (3) dilutor test tube; (4) air dilution pipe; (5) hot diluted sample; (6) way out undiluted aerosol; (7) thermodilutor; (8) particle free and dry dilution air; (9) sample entry to EEPS; (10) EEPS; (11) flow meter; (12) on-board measurement system [14].

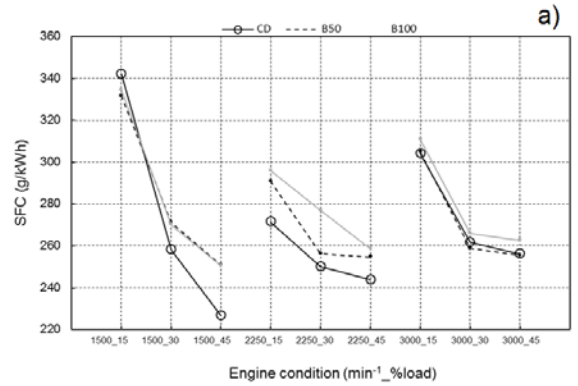
a)
CD
B50
B100
SFC (g/kWh)
360
340
320
300
280
260
240
220
1500_15 1500_30 1500_45 2250_15 2250_30 2250_45 3000_15 3000_30 3000_45
Engine condition (min-1_%load)

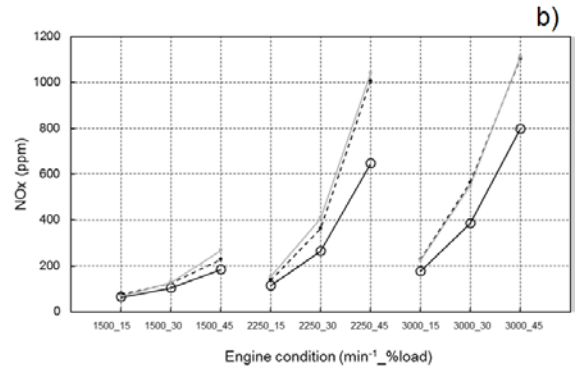
b)
NOx (ppm)
1200
1000
800
600
400
200
0
1500_15 1500_30 1500_45 2250_15 2250_30 2250_45 3000_15 3000_30 3000_45
Engine condition (min-1_%load)

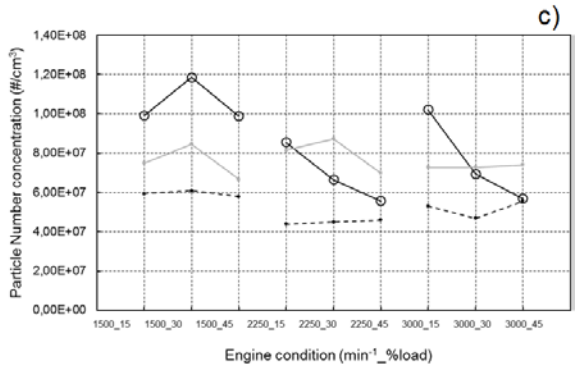
c)
Particle Number concentration (#/cm3)
1,40E+08
1,20E+08
1,00E+08
8,00E+07
6,00E+07
4,00E+07
2,00E+07
0,00E+00
1500_15 1500_30 1500_45 2250_15 2250_30 2250_45 3000_15 3000_30 3000_45
Engine condition (min-1_%load)

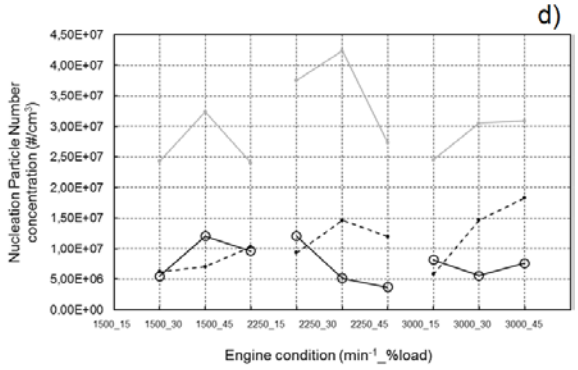
d)
Nucleation Particle Number concentration (#/cm3)
4,50E+07
4,00E+07
3,50E+07
3,00E+07
2,50E+07
2,00E+07
1,50E+07
1,00E+07
5,00E+06
0,00E+00
1500_15 1500_30 1500_45 2250_15 2250_30 2250_45 3000_15 3000_30 3000_45
Engine condition (min-1_%load)

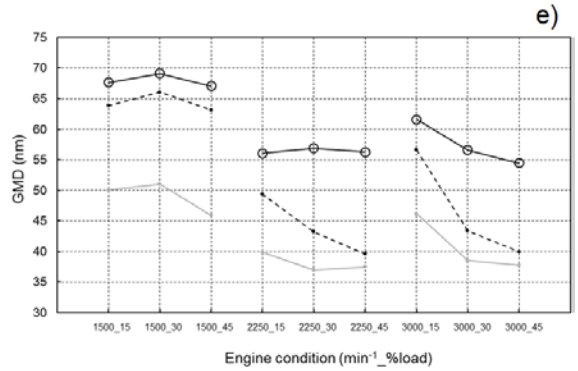
e)
GMD (nm)
75
70
65
60
55
50
45
40
35
30
1500_15 1500_30 1500_45 2250_15 2250_30 2250_45 3000_15 3000_30 3000_45
Engine condition (min-1_%load)

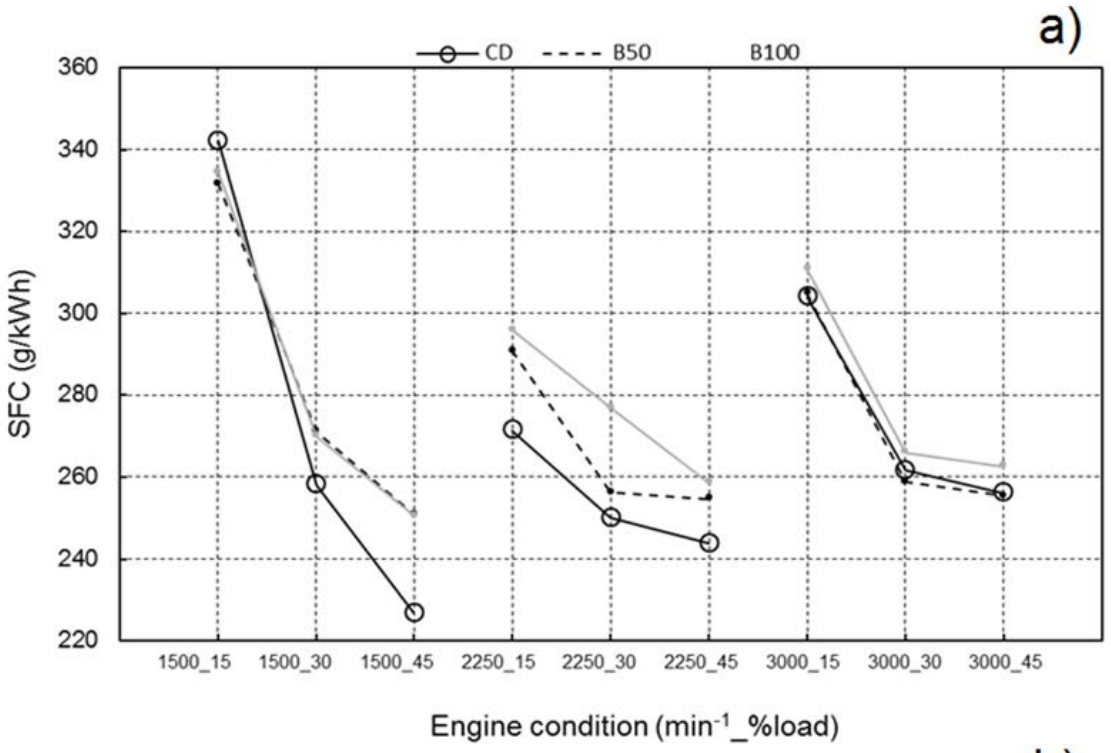
a)
CD
B50
B100
SFC (g/kWh)
360
340
320
300
280
260
240
220
1500_15
1500_30
1500_45
2250_15
2250_30
2250_45
3000_15
3000_30
3000_45
Engine condition (min-1_%load)

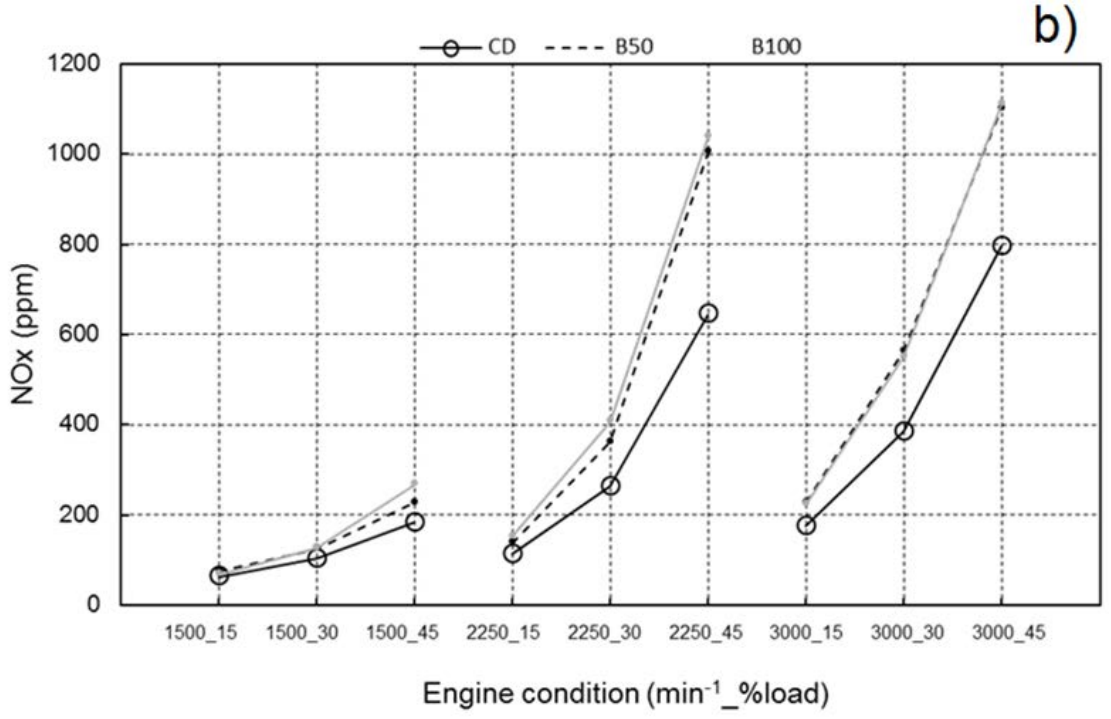
b)
CD
B50
B100
NOx (ppm)
1200
1000
800
600
400
200
0
1500_15
1500_30
1500_45
2250_15
2250_30
2250_45
3000_15
3000_30
3000_45
Engine condition (min-1_%load)

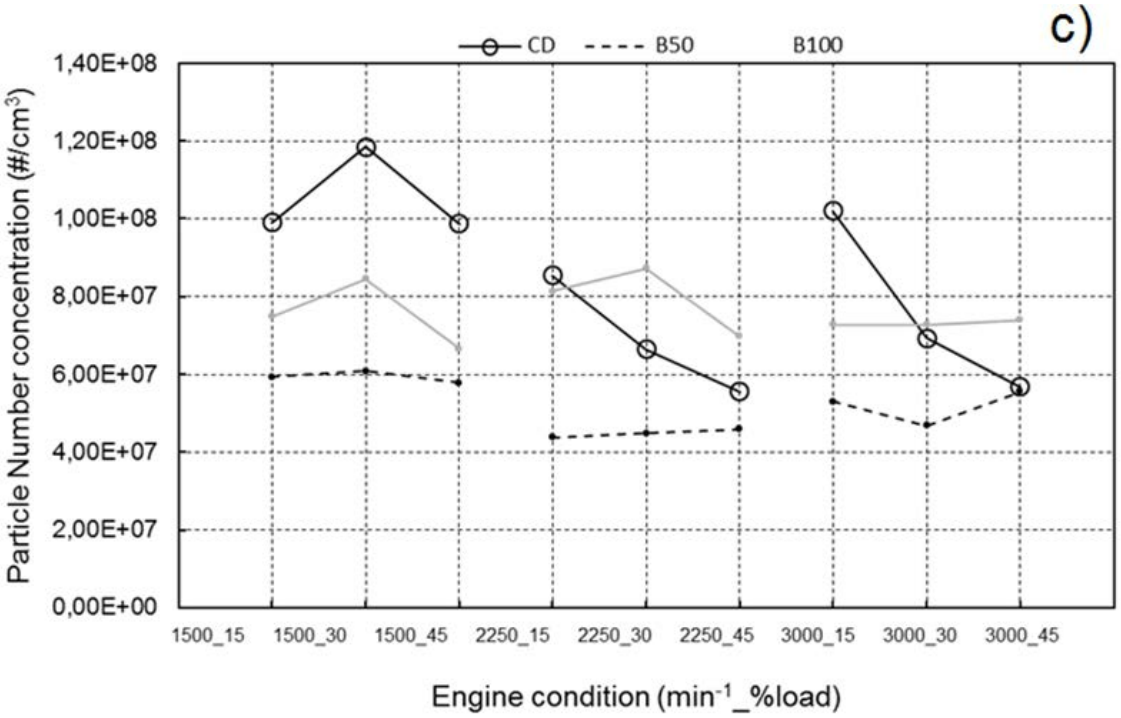
c)
CD
B50
B100
Particle Number concentration (#/cm3)
1,40E+08
1,20E+08
1,00E+08
8,00E+07
6,00E+07
4,00E+07
2,00E+07
0,00E+00
1500_15
1500_30
1500_45
2250_15
2250_30
2250_45
3000_15
3000_30
3000_45
Engine condition (min-1_%load)

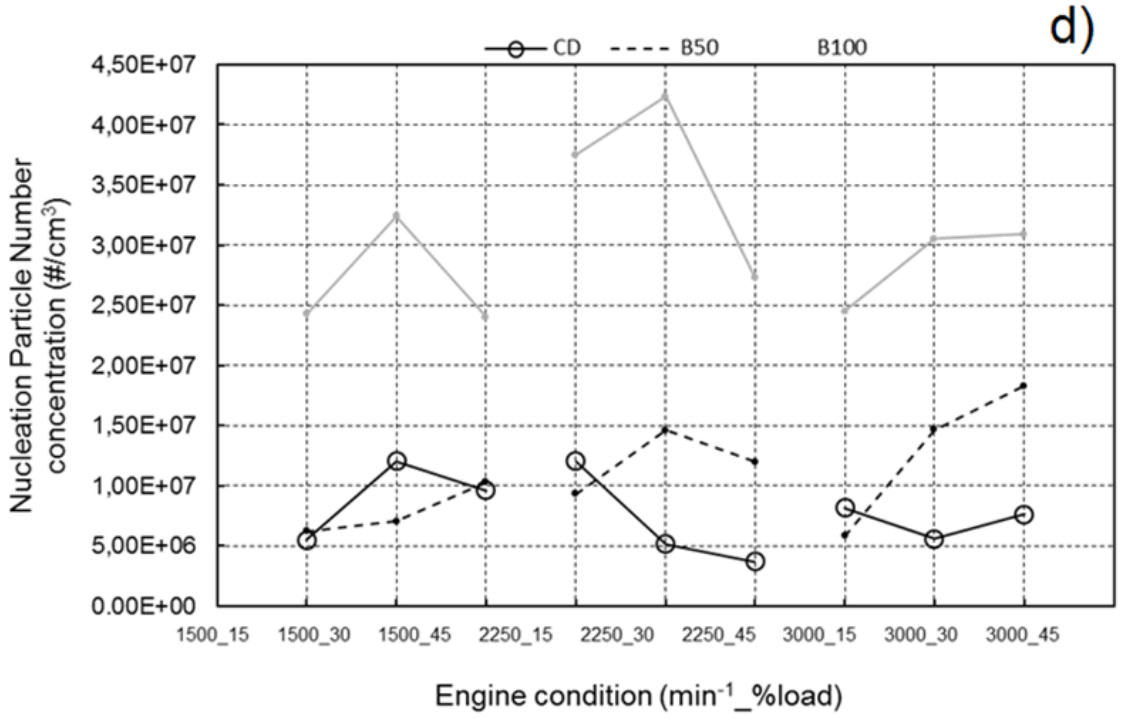
d)
CD
B50
B100
Nucleation Particle Number concentration (#/cm3)
4,50E+07
4,00E+07
3,50E+07
3,00E+07
2,50E+07
2,00E+07
1,50E+07
1,00E+07
5,00E+06
0.00E+00
1500_15
1500_30
1500_45
2250_15
2250_30
2250_45
3000_15
3000_30
3000_45
Engine condition (min-1_%load)

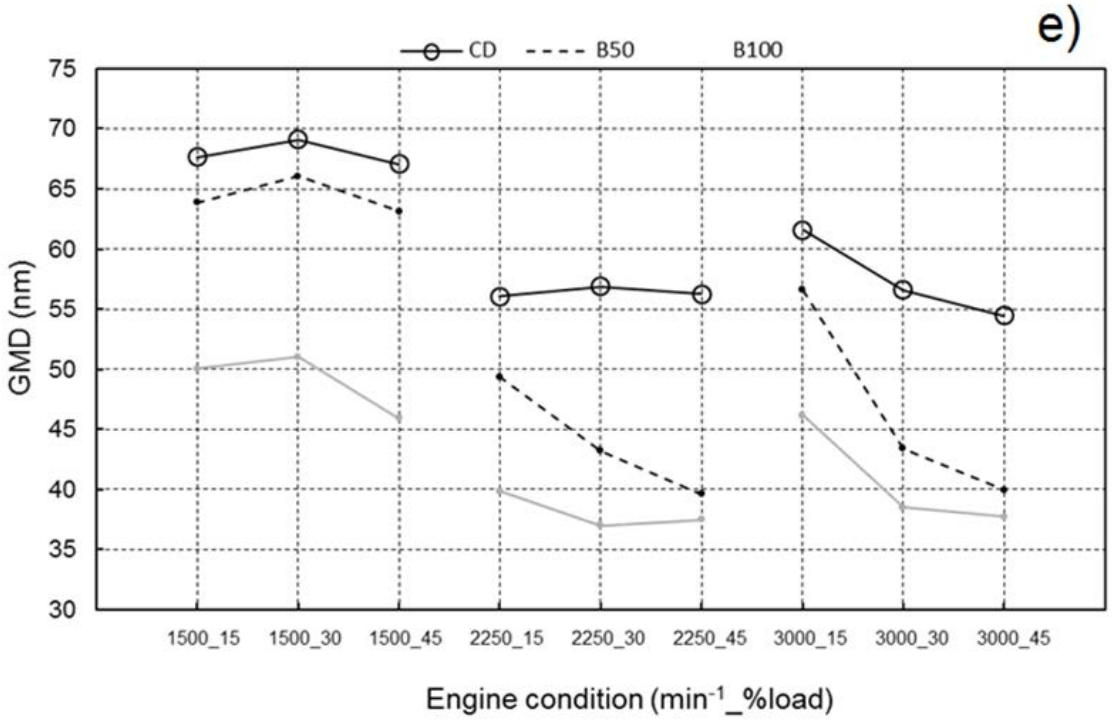

Figure 4. Values of a) SFC, b) NOx, c) Total particle number, d) Nucleation mode particle number and e) GMD for different engine conditions.

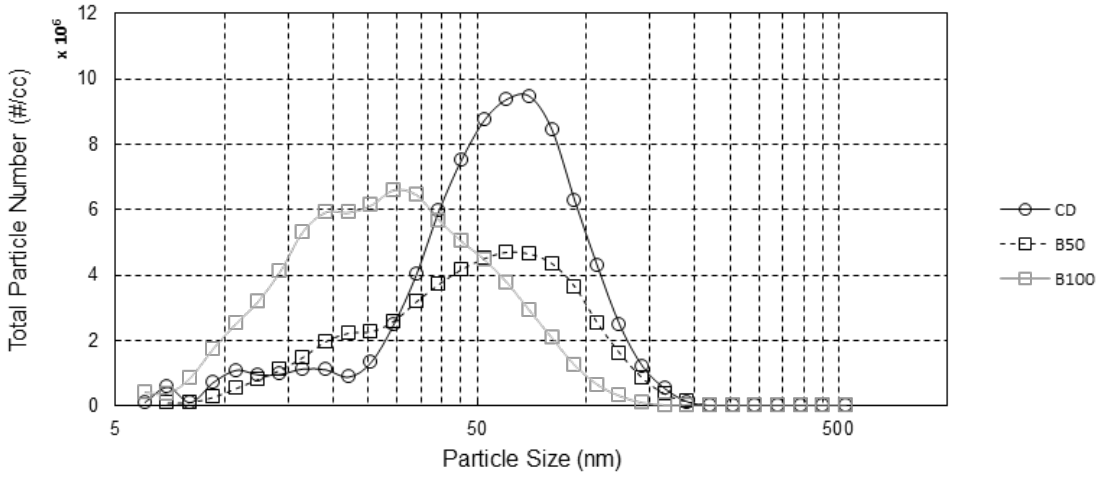

Figure 5. Particle size distribution for CD, B50 and B100 at 3000 min^{-1} and 45% load.

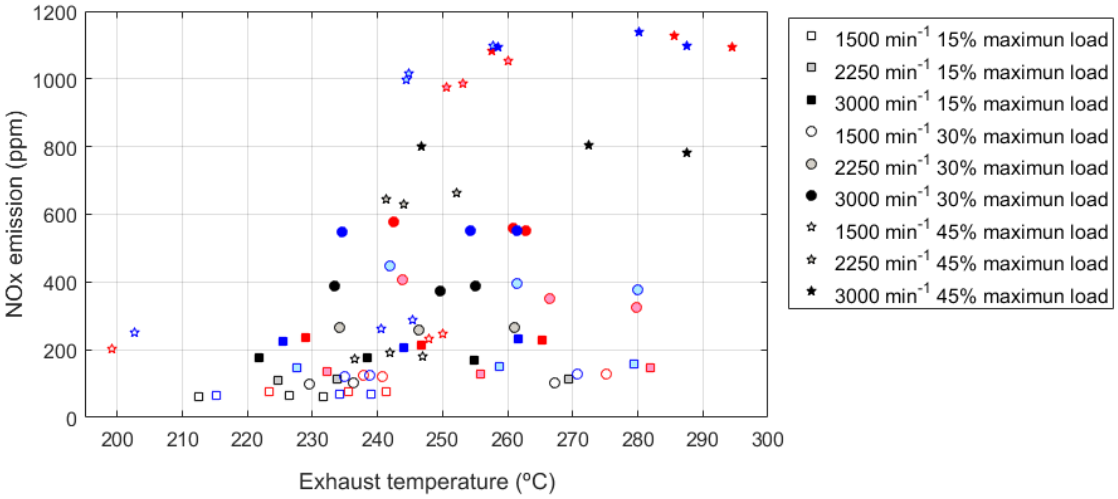

Figure 6. NOx emission depending on exhaust temperature, engine operating condition and fuel (black CD; red B50; blue B100)